Talanta 111 (2013) 206–214

Contents lists available at SciVerse ScienceDirect

Talanta

journal homepage: www.elsevier.com/locate/talanta

Manipulating ionic strength to improve single cell electrophoretic separations

Richard B. Keithley, Mark P. Metzinger, Andrea M. Rosado, Norman J. Dovichi *

Department of Chemistry and Biochemistry, University of Notre Dame, Notre Dame, IN 46556, USA

ARTICLE INFO

Article history:
Received 25 January 2013
Received in revised form
1 March 2013
Accepted 4 March 2013
Available online 13 March 2013

Keywords:
Capillary electrophoresis
Laser-induced fluorescence
Single cell analysis

ABSTRACT

A capillary electrophoresis system with ultrasensitive two-color laser-induced fluorescence detection was used to probe the effect of ionic strength on single cell separations of glycosphingolipids. Differentiated PC12 cells were incubated with two ganglioside substrates tagged with different fluorophores within the BODIPY family such that two distinct metabolic patterns could be simultaneously monitored. Aspiration of single differentiated PC12 cells suspended in a phosphate-buffered saline solution showed excessive peak dispersion, poor resolution, and peak efficiencies below 100,000 theoretical plates. Aspiration of single differentiated PC12 cells suspended in deionized water corrected peak dispersion. Average peak efficiencies ranged between 400,000 and 600,000 theoretical plates. Improved performance was due to the dilution of the high salt concentrations inside of single neuronal-like cells to produce field amplified sample stacking. Single cell separations showed the highest resolution when aspiration of single differentiated PC12 cells suspended in deionized water were separated using a running buffer of high ionic strength. The improvement in resolution allowed for the identification of analytes not previously detected in single cell metabolism studies.

1. Introduction

Traditional biological assays utilize aggregate analysis of thousands of cells to study biomolecules of interest. However, this approach eliminates the ability of researchers to study inherent variation among single cells. Even genetically identical cells can display differences in their content due to differences in cell size, cell density within tissue, and differences in their local environment [1,2]. Single cell analysis has been used in studies within the fields of neuroscience [3,4], oncology [5], enzymology [6,7], immunology [8], and genetics [9]. A variety of analytical detection methods have been used to characterize single cells including electrochemistry, mass spectrometry, and fluorescence [10]. Capillary electrophoresis (CE) has been used to separate the contents of single cells since the late 1980s [4,11]. CE offers improvements in single cell analysis due to its small volume requirements and fast, efficient separations [12].

Glycosphingolipids (GSLs) are amphiphilic molecules that are present in moderate concentrations within neuronal cell membranes [13]. GSLs contain a polar headgroup consisting of a diverse suite of carbohydrates combined with a hydrophobic tail composed of a fatty acid and a sphingosine (termed ceramide). Gangliosides are a specific subtype of GSLs that contain at least one sialic acid in the polar headgroup. Gangliosides are involved in a variety of cell functions including cell signaling and differentiation [14–21]. Studying GSL metabolism is of great interest because defects in GSL metabolism play a role in several disorders such as Tay–Sachs Disease and seizure conditions [22–25]. A simplified overview of GSL metabolism is shown in Fig. 1A.

Our group developed the technique termed “metabolic cytometry” that utilizes CE combined with laser-induced fluorescence to study metabolism within single cells [26]. In this approach, cells are incubated with a GSL substrate that has a fluorescent tag covalently bound to its ceramide tail. Carriers such as artificial lipid vesicles [27], de-fatted bovine serum albumin [28], or cyclodextrins [29] are added to the cellular medium to enhance delivery, transfer, and insertion of these fluorescent GSLs into cells. Once inside, these fluorescent GSLs are trafficked and metabolized intracellularly where endogenous anabolic and catabolic enzymes can add and remove (respectively) various sugar moieties within the headgroup [30]. While metabolism occurs within the headgroup of the exogenously added fluorescent GSL, the fluorophore on the ceramide tail remains intact and all metabolic products of the fluorescent substrate will be fluorescent. To assess metabolism, a single cell is then aspirated into a capillary, lysed, and the fluorescently-labeled GSLs are separated by CE with laser-induced fluorescence detection. Cells can also be simultaneously incubated with multiple GSLs labeled with different fluorophores; instruments are then constructed with multiple excitation sources to monitor multiple metabolic pathways in the same cells at the same time [31,32].

Buffer composition plays a pivotal role in the quality of GSL separations by CE. In capillary zone electrophoresis (CZE),

* Corresponding author. Tel.: +1 574 631 2778; fax: +1 574 631 6652.
E-mail address: Norman.J.Dovichi.1@nd.edu (N.J. Dovichi).

0039-9140/$ - see front matter © 2013 Elsevier B.V. All rights reserved.
http://dx.doi.org/10.1016/j.talanta.2013.03.012

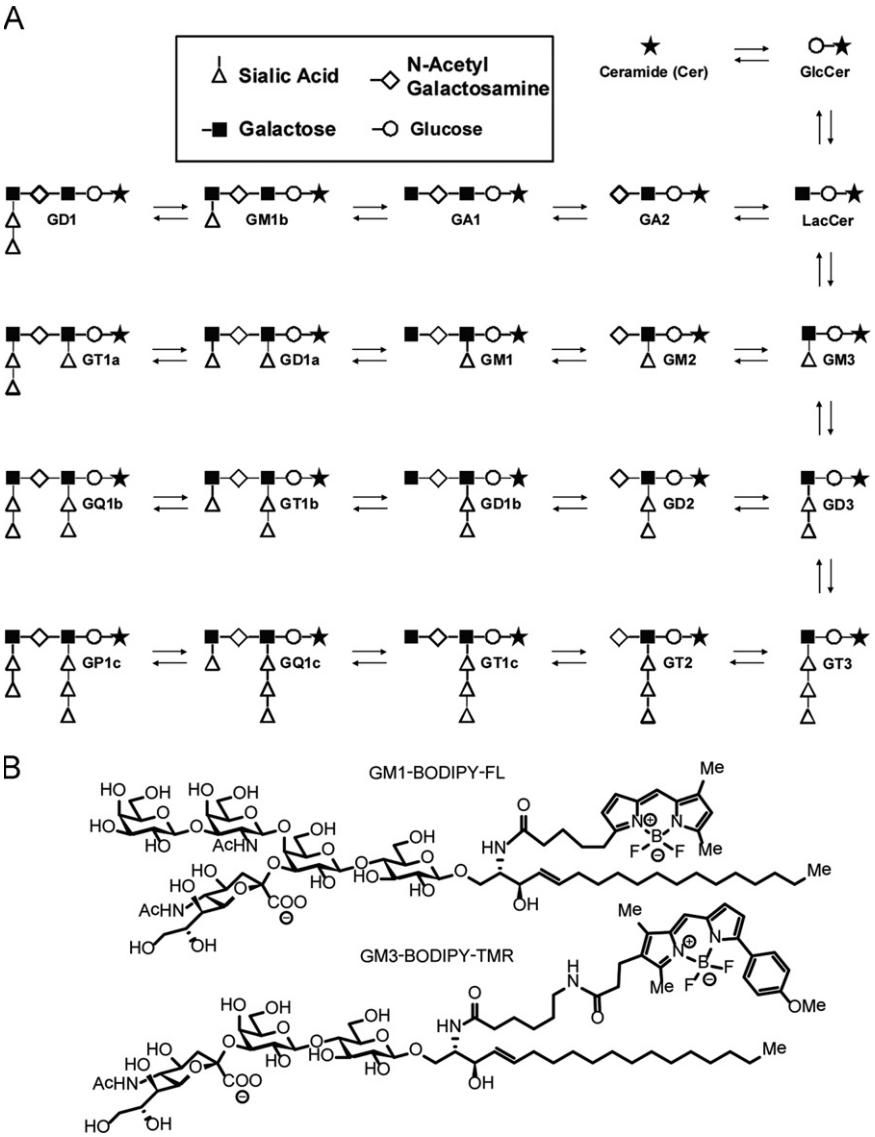

Fig. 1. (A) Simplified schematic of GSL metabolism. (B) Structures of the synthetically prepared GM1-BODIPY-FL and GM3-BODIPY-TMR substrates.

borate/phosphate buffers containing the additive α-cyclodextrin (α-CD) have been used to separate GSLs [33–35]. The ionic strength of the separation buffer can also affect the separation of GSLs [36]. In CZE-based separations, buffers with low ionic strengths are preferred because increases in the ionic strength have been shown to cause peaks shapes to become more asymmetric as the migration times increase [36]. CZE is not a preferred method of separating GSLs because the amphiphilic nature of GSLs causes them to form heterogeneous multi-analyte mixed micelles in solution [37], confounding their detection [36]. In micellar electrokinetic capillary chromatography (MECC), the presence of surfactant breaks up these mixed micelles and generally yields very high peak efficiencies (>400,000 theoretical plates) [38].

Varieties of experimental and instrumental approaches have been used to improve single cell electrophoretic separations focusing on sample preparation, sample manipulation, and cellular lysis. The cell suspension solution should both maintain cell integrity while also preventing cell lysis, allowing for an intact cell to be injected into the capillary [11]. When studying single cell metabolism, fixation of the cells is needed to arrest their metabolic profiles at the time of harvesting to eliminate artifacts associated with storing the cells long-term [36]. The manual isolation of a single cell and introduction of that cell into the capillary also affects analyte separation [39]. Intact cells are traditionally introduced into the capillary using negative pressure and lysed once inside to release their contents [12,39,40]. In addition, the inner diameter of the capillary influences the injection of a single cell. Having an etched capillary tip similar to the size of the cell to be separated can improve the injection of a single cell into the capillary [12]. The running buffer can be used to both lyse the cell and separate the components inside the cell [12]. Otherwise, plugs of detergent such as sodium dodecylsulfate (SDS) can be aspirated to assist in cell lysis [41].

Here, we demonstrate that the manipulation of ionic strength can also be used to improve the quality of single cell separations. The PC12 cell line, originating from rat adrenal tissue, was used as a model neuronal system. Upon addition of neuronal growth factor (NGF), PC12 cells differentiate into neuronal-like cells (dPC12s) [42]. dPC12 cells were incubated with two fluorescent GSL substrates shown in Fig. 1B, GM1-BODIPY-FL ($\lambda_{ex}/\lambda_{em}$ 505 nm/513 nm) [43] and GM3-BODIPY-TMR ($\lambda_{ex}/\lambda_{em}$ 542 nm/574 nm) [43]. GSL metabolism was then monitored in single cells using capillary electrophoresis with two-color laser-induced fluorescence detection.

2. Materials and methods

2.1. Capillary electrophoresis with two-color laser induced fluorescence detection

The capillary electrophoresis system was a modified version of those previously described [31,44]. A high voltage power supply (Spellman CZE1000R, Hauppauge, NY) was used to generate the electrophoretic voltage. Fluorescence detection was measured in a sheath flow cuvette (Hellma USA, Plainview, NY) [45]. All separations were performed using MECC on a fused-silica capillary 45 cm in length, 30 μm inner diameter, and 150 μm outer diameter (Polymicro Technologies, Phoenix, AZ).

All optical components were purchased from Thorlabs (Newton, NJ) and CVI Melles Griot (Albuquerque, NM) unless otherwise noted. Solid state diode lasers, 473 nm (Lasermate, Walnut, CA) and 532 nm (CrystaLaser, Reno, NV), were both operated at a power of 10 mW. The 473 nm and 532 nm beams were focused approximately 50 μm and 70 μm downstream from the distal end of the capillary, respectively. The beams were offset from each other to minimize photobleaching and scatter [31,32]. Emission was collected with a 0.7 N.A. microscope objective (Universe Kogaku, Oyster Bay, NY) and then passed through a 567 nm dichroic beam splitter. Green emission from the BODIPY-FL-labeled GSLs was reflected, filtered (510DF10 bandpass), and carried by a fiber optic cable to a multi-channel SPCM-AQ4C single-photon counting avalanche photodiode detector (APD) (Excelitas Technologies, Waltham, MA). Orange emission from the BODIPY-TMR-labeled GSLs was passed through the 567 nm dichroic, filtered (580DF20 bandpass), and carried by a fiber optic cable coupled to the APD.

Unless otherwise noted, all chemicals used were purchased from Sigma Aldrich (St. Louis, MO). Four buffer compositions were used for this work, all made in 18.2 MΩ distilled deionized water (dH_2O, Barnstead Nanopure System, Thermo Scientific, Waltham, MA) and were filtered twice (0.2 μm) before use. One contained 100 mM TRIS, 100 mM CHES (Alfa Aesar, Ward Hill, MA), 20 mM SDS, and 5 mM α-CD (Alfa Aesar). Another buffer contained 25 mM TRIS, 25 mM CHES, 20 mM SDS, and 5 mM α-CD. A third buffer contained 250 mM TRIS, 250 mM CHES, 20 mM SDS, and 5 mM α-CD. Finally, a fourth buffer contained 10 mM sodium tetraborate, 35 mM sodium deoxycholate, and 5 mM methyl-β-CD. A separation voltage of 26 kV was used for all TRIS/CHES/SDS/α-CD formulations while 18 kV was used for the borate/deoxycholate/methyl-β-CD buffer.

Data was acquired with a custom LabVIEW program (PCI-6035E and PCI-6602 cards, National Instruments, Austin, TX) at a rate of 50 Hz. Data was analyzed using Origin (OriginLab Corporation, Northampton, MA), Igor (WaveMetrics, Portland, OR), and LabVIEW. Electropherograms were corrected for the 56 ns APD dead time [46]. After dead time correction, the signal was passed through a 5 point median filter. Because of peak dispersion, separation efficiencies (N_{SYS}) were calculated using

$$N_{SYS} = \frac{41.7(t_R/W_{0.1})^2}{B/A+1.25} \quad (1)$$

where t_R was the migration time, $W_{0.1}$ was the peak width at 10% of the maximum height, and B/A represents the asymmetry factor of the peak [47]. Resolution (R) was calculated using

$$R = \frac{2(t_2-t_1)}{W_1+W_2} \quad (2)$$

where t_1 and t_2 are the migration times of the two species and W_1 and W_2 are their corresponding base peak widths.

2.2. Sample preparation

2.2.1. Cell culture

Rat PC12 cells (strain CRL-1721) were purchased from American Type Culture Collection (ATCC, Manassas, VA). Rat-tail collagen I (Life Technologies) was used to coat flasks according to the manufacturer's instruction because PC12 cells adhere poorly to plastic [42]. The cells were grown in RPMI 1640 medium (ATCC) supplemented with 5% fetal bovine serum, 10% horse serum, 2 mM GlutaMAX, and a mixture of amphotericin B, streptomycin, and penicillin (Life Technologies). PC12 cells were reseeded on flasks coated with mouse collagen IV according to the manufacturer's instructions (BD Biosciences) for differentiation and lipid incubation. The RPMI 1640 culture medium was then supplemented with 50 ng/mL NGF (BD Biosciences, San Jose, CA) to differentiate the PC12 cells into neuronal like cells [42].

2.2.2. Lipid incubation

The GM1-BODIPY-FL and GM3-BODIPY-TMR substrates were prepared as previously described [32]. Prior to lipid incubation, dPC12 cells were grown in RPMI 1640 medium supplemented with NGF for 10 days. Cells were washed with calcium- and magnesium-free PBS (2.67 mM KCl, 1.47 mM KH_2PO_4, 8.06 mM $Na_2HPO_4{\cdot}7H_2O$, 137.93 mM NaCl, Life Technologies). The medium was replaced with serum free, NGF-supplemented RPMI 1640 medium (RPMI 1640, 2 mM GlutaMAX, amphotericin B, streptomycin, penicillin, 50 ng/mL NGF) for 2 days before the introduction of fluorescently labeled lipids so that dPC12 cells could adjust to the serum-free environment. A serum-free environment is needed to enhance delivery of the amphiphilic fluorescent GSLs into cells otherwise the fluorescent GSLs can instead preferentially partition into the large excess of lipoproteins present in serum [30]. GM1-BODIPY-FL and GM3-BODIPY-TMR were reconstituted in biological grade ethanol and complexed with a methyl-β-CD carrier at a 1:1.5 lipid to CD ratio to assist in GSL delivery into dPC12 cells. Cell culture medium was then added so the final concentration of each of the fluorescent GSL substrates was 2 μM. dPC12 cells were incubated with culture medium containing the fluorophores for 30 min, washed with PBS, then incubated with serum free NGF-supplemented RPMI 1640 medium for an additional 23.5 h. Cells were removed using a 0.25% trypsin/EDTA solution (Life Technologies). Trypsin was deactivated using soybean trypsin inhibitor (Sigma Aldrich). Cells were washed with PBS and fixed using a 4% paraformaldehyde solution. The fixation process was quenched using 10 mM glycine in PBS for 30 min. Cells were again washed with PBS and stored in PBS at 4 °C until use. For homogenate analysis, cells were lysed in 1% SDS in PBS (w/v) in lieu of the fixation protocol.

2.3. Single cell experimentation

2.3.1. Cell introduction into the capillary

Cell injection was carried out under an Olympus IX70 inverted light microscope (Olympus, Tokyo, Japan). A suspension of dPC12 cells (5 μL) was first placed on a glass slide. The capillary was lowered and positioned with a micromanipulator (Soma Scientific, Irvine, CA) such that the inner diameter of the capillary surrounded a single cell [41]. Single cells were injected hydrodynamically by applying approximately 11 kPa of negative pressure at the terminus of the capillary for four seconds. In instances where single cells were sandwiched between plugs of solution, the tip of the injection end of the capillary was placed in the desired solution and negative pressure was applied at the distal end of the capillary before and after the injection of a single dPC12 cell. Each single cell rested within the injection end of the capillary for

2 min before the separation voltage was applied. Peak identity in the single cell separations was confirmed by running bulk cell homogenates and spiking in known single-analyte standards.

2.3.2. Separation conditions

Several conditions were used to improve the quality of the single cell separations in the TRIS/CHES/SDS/α-CD buffer formulation (vide infra) as shown in Fig. 2. In condition A, a single dPC12 cell suspended in PBS was injected onto the capillary, surrounded by plugs of 1% SDS (w/v) in PBS. Separations were performed in 100 mM TRIS, 100 mM CHES, 20 mM SDS, and 5 mM α-CD. In condition B, a single dPC12 cell suspended in PBS was simply injected onto the capillary and separations were performed in 100 mM TRIS, 100 mM CHES, 20 mM SDS, and 5 mM α-CD. For condition C, a single dPC12 cell suspended in PBS was injected onto the capillary surrounded by plugs of DNA-*Zap*™ solution (Life Technologies). Separations were carried out in 100 mM TRIS, 100 mM CHES, 20 mM SDS, and 5 mM α-CD. In condition D, a suspension of dPC12 cells in PBS was diluted ten-fold with dH_2O. A single dPC12 cell suspended in this deionized water solution was hydrodynamically injected into the capillary and separations were carried out in 100 mM TRIS, 100 mM CHES, 20 mM SDS, and 5 mM α-CD. In condition E, a single dPC12 cell suspended in PBS was injected onto the capillary and separations were carried out in 25 mM TRIS, 25 mM CHES, 20 mM SDS, and 5 mM α-CD. In condition F, a single dPC12 cell suspended in PBS was injected onto the capillary and separations were carried out in 250 mM TRIS, 250 mM CHES, 20 mM SDS, and 5 mM α-CD. Finally, in condition G, single dPC12 cells were diluted in dH_2O as in condition D and separations were performed using a 250 mM TRIS, 250 mM CHES, 20 mM SDS, and 5 mM α-CD buffer.

Two other single cell conditions were tested using a 10 mM sodium tetraborate, 35 mM sodium deoxycholate, and 5 mM methyl-β-CD buffer formulation. In one approach, a single dPC12 cell suspended in PBS was injected onto the capillary. In another approach, single dPC12 cells suspended in PBS were diluted ten-fold with dH_2O. A single dPC12 cell suspended in the deionized water solution was then injected onto the capillary and the separation was performed.

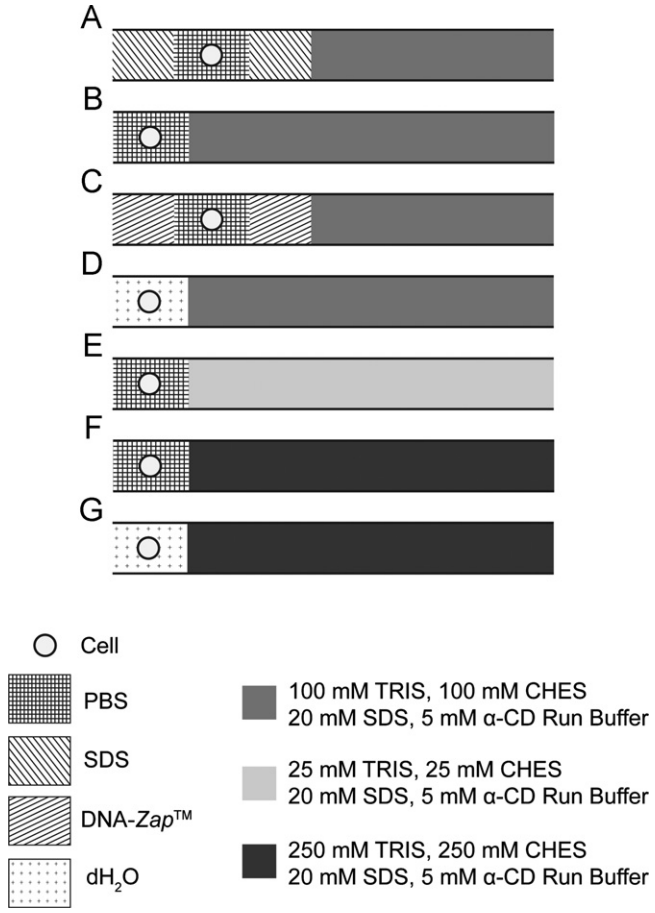

Fig. 2. Summary of conditions used in the analysis of GSL metabolism in single dPC12 cells. (A) A single dPC12 cell, suspended in PBS and bracketed between two plugs of 1% SDS in PBS, was separated using a 100 mM TRIS, 100 mM CHES, 20 mM SDS, and 5 mM α-CD buffer. (B) A single dPC12 cell suspended in PBS was separated using a 100 mM TRIS, 100 mM CHES, 20 mM SDS, and 5 mM α-CD buffer. (C) A single dPC12 cell, suspended in PBS and bracketed between two plugs of DNA-*Zap*™, was separated using a 100 mM TRIS, 100 mM CHES, 20 mM SDS, and 5 mM α-CD buffer. (D) A single dPC12 cell diluted in dH_2O was separated using a 100 mM TRIS, 100 mM CHES, 20 mM SDS, and 5 mM α-CD buffer. (E) A single dPC12 cell suspended in PBS was separated using a 25 mM TRIS, 25 mM CHES, 20 mM SDS, and 5 mM α-CD buffer. (F) A single dPC12 cell suspended in PBS was separated using a 250 mM TRIS, 250 mM CHES, 20 mM SDS, and 5 mM α-CD buffer. (G) A single dPC12 cell suspended in dH_2O was separated using a 250 mM TRIS, 250 mM CHES, 20 mM SDS, and 5 mM α-CD buffer.

3. Results and discussion

3.1. Two-color metabolic cytometry

The neuronal-like dPC12 cells were incubated with the GM1-BODIPY-FL and GM3-BODIPY-TMR fluorescent substrates (Fig. 1B). These fluorescent GSLs were trafficked intracellulary where they were metablized by endogenous enzymes present in various locations including the Golgi complex and lysosomes. dPC12 cells were allowed to metabolize these fluorescent substrates for 24 h. Because the fluorophores were present on the hydrophobic ceramide tail of GSLs, all subsequent metabolic products due to the addition (such as anabolism in the Golgi) or removal (such as catabolism within the lysosome) of carbohydrates from the polar headgroup also fluoresced. After 24 h, the dPC12 cells were formaldehyde fixed and the metabolic profiles of single cells were determined using MECC with two-color laser-induced fluorescence detection. A single dPC12 cell suspended in a solution of PBS, placed between plugs of 1% SDS to ensure cell lysis, was aspirated into a capillary filled with 100 mM TRIS, 100 mM CHES, 20 mM SDS, and 5 mM α-CD running buffer (hereon abbreviated as TCS-α) using negative pressure (Fig. 2A).

The separation gave broad, fronted peaks for all species in both channels with inadequate resolution between peaks as shown in the representative trace Fig. 3A (enlargement shown in Fig. 3a). As an example, GM1-BODIPY-FL was not baseline resolved from its catabolic metabolite GM2-BODIPY-FL in any of the single cell electropherograms ($N=6$ cells). While the quality of the separation was mediocre, some peaks could be identified as the products of GSL metabolism shown in Fig. 1A. GM1-BODIPY-FL underwent catabolism to produce the smaller, more hydrophobic products GM2-BODIPY-FL and Cer-BODIPY-FL which migrated after GM1-BODIPY-FL. The presence of a shoulder on the fronted GM1-BODIPY-FL peak could indicate that GM1-BODIPY-FL also underwent anabolism to produce larger, more hydrophilic products that migrated earlier in the MECC-based separation, but the poor quality of the separation prevented analyte identification. GM3-BODIPY-TMR underwent catabolism to produce LacCer-BODIPY-TMR and Cer-BODIPY-TMR. GM3-BODIPY-TMR also underwent anabolism to produce more hydrophilic products that migrated earlier in the separation (between 7.2 and 7.5 min), but the resolution of the separation was not sufficient to allow for analyte identification.

Peak efficiencies were calculated for each channel using GM1-BODIPY-FL and Cer-BODIPY-TMR (Eq. (1)). The average results

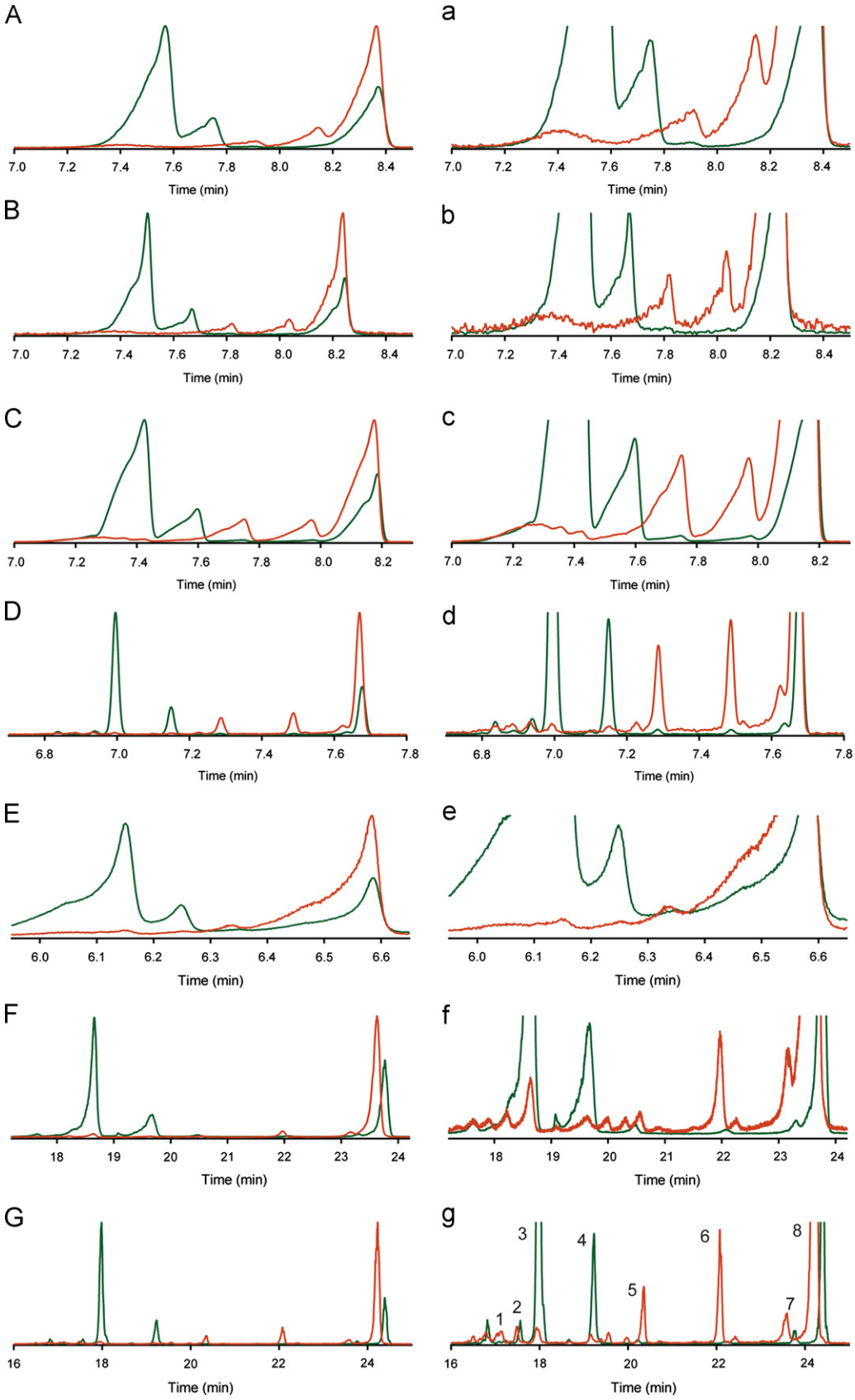

Fig. 3. Two-color electropherograms of GSL metabolism in single dPC12 cells. Electropherograms A–G were taken under the A–G operating conditions, respectively, described in Fig. 2. Electropherograms a–g represent enlargements of corresponding electropherograms A–G. In each graph, the abscissa represents migration time while the ordinate is in units of fluorescence (Hz). Green and orange traces correspond to the BODIPY-FL and BODIPY-TMR channels, respectively. A running voltage of 26 kV was used for all separations. The numbered labels correspond to GSLs GT1a/b (1), GD1a/b (2), GM1 (3), GM2 (4), GM3 (5), LacCer (6), GlcCer (7), and Cer (8). (For interpretation of the references to color in this figure legend, the reader is referred to the web version of this article.)

taken from several two-color single cell electropherograms are presented in Fig. 4. Average peak efficiencies were approximately an order of magnitude lower than previously reported [31]. We have demonstrated peak efficiencies in the range of 400,000–600,000 theoretical plates for these same analytes in primary rat neurons and glia using a buffer consisting of 10 mM sodium tetraborate, 35 mM sodium deoxycholate, and 5 mM methyl-β-CD (hereon abbreviated as 10/35/5) [31].

Interestingly, separations in TCS-α buffer have been shown to be more efficient than those in 10/35/5 buffer in the analysis of single fluorescent GSL standards [38]. While both buffers utilize MECC-based separations, the mechanism of GSL separation is different between the buffers, which may explain why the TCS-α buffer outperforms the 10/35/5 buffer in the analysis of single GSL standards, but not single cell separations. In addition to improved peak efficiencies, TCS-α also lowers the current across the capillary, dramatically improves resolution between complex GSLs, and offers a lower limit of detection, which are critical advantages that allow for the analysis of the small amounts of material present in single cells [38]. In an effort to improve separations and recoup many of the advantages inherent to the TCS-α buffer, running conditions were altered in various ways.

Single cells are traditionally surrounded by plugs of surfactant to ensure cell lysis before applying the separation voltage [41,44,48]. However, here the running buffer contained approximately 0.5% SDS which is sufficient to lyse cells in less than 2 s [49]. Therefore, instead of surrounding single dPC12 cells between two plugs of detergent, the running buffer was allowed to lyse the cells. Approximately 2 min after aspiration of the single cell suspended in PBS into a capillary filled with TCS-α buffer, the running voltage was applied to begin the separation (Fig. 2B). A representative two-color single dPC12 cell electropherogram under these conditions is shown in Fig. 3B (blowup in Fig. 3b). Peaks were still broad, peak efficiencies did not significantly change (Fig. 4), and again, none of the single cell electropherograms showed baseline resolution between GM1-BODIPY-FL and its metabolite GM2-BODIPY-FL ($N=5$). Because these data were not significantly different from those taken using plugs of 1% SDS, the surfactant present in the MECC buffer was sufficient to lyse single cells and plugs of detergent were no longer used to assist in cell lysis.

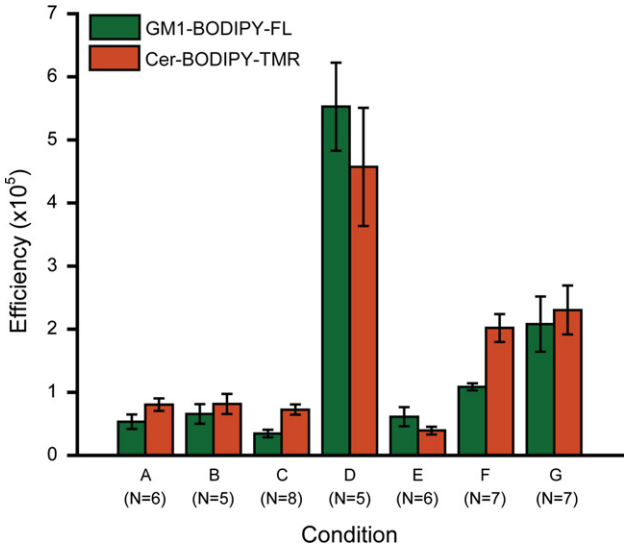

Fig. 4. GM1-BODIPY-FL (green) and Cer-BODIPY-TMR (orange) peak efficiencies under each of the separation conditions described in Fig. 2. *N* is the number of single cells analyzed with each separation condition. (For interpretation of the references to color in this figure legend, the reader is referred to the web version of this article.)

While only the fluorescently tagged GSLs are measured, other cellular components are also solubilized when a single dPC12 cell is injected into the capillary and lysed that could impact the separation. To investigate the impact of oligonucleotides on the separation, a single dPC12 cell suspended in PBS buffer was bracketed between plugs of DNA-*Zap*™ (Fig. 2C). DNA-*Zap*™ is a commercially available solution intended to decontaminate PCR thermocyclers that rapidly degrades DNA and RNA into nucleotides on contact [50]. Encompassing single dPC12 cells between plugs of DNA-*Zap*™ did not improve the quality of the separation as shown in Fig. 3C and c. GM1-BODIPY-FL and GM2-BODIPY-FL were not baseline resolved in any of the single cell electropherograms ($N=8$) and peak efficiencies did not improve in either channel (Fig. 4). This result indicates that the presence of DNA and RNA did not significantly contribute to the poor quality of the single sell separations.

3.2. Stacking to improve single cell capillary electrophoresis

Interestingly, all the peaks in the single cell electropherograms presented thus far appear heavily fronted. Fronting in capillary electrophoresis usually occurs when an analytes of higher mobility than buffer ions are injected onto the capillary in a high conductivity (high ionic strength) solution [51]. While the ionic strength of the PBS used for the single cell suspension is less than that of the TCS-α running buffer (see Section 2), the ionic composition of the single cells may play a role. Indeed, neuronal cells contain potassium ions at concentrations of hundreds of millimolar to allow for the induction of voltage propagations termed action potentials used in neuronal communication [52]. The neuronal-like dPC12 cells are also known to have high concentrations of intracellular potassium [53]. The contents of a single cell (approximately 5 pL in total volume) are greatly diluted upon lysis inside of the sample region of the capillary (approximately 1 nL) [41]. However, it is still possible that local regions of high ionic strength (low electric field) exist which could favor peak fronting, especially with the small amounts of fluorescent GSLs contained within single cells and the 2 min waiting time used to ensure cell lysis.

Single dPC12 cells originally suspended in PBS were diluted in dH_2O and aspirated into the capillary to determine if ionic strength played a role in the peak dispersions recorded under other separation conditions (Fig. 2D). The dilution of analyte in dH_2O is traditionally used for field amplified sample stacking [54], a way to improve concentration detection limits in electrophoretic separations [55]. Low ionic strength cell suspensions can also assist in cell lysis in single cell electrophoretic separations [40]. However, because the dPC12 cells were formaldehyde-fixed prior to analysis, cells did not lyse when stored in this solution.

A representative two-color single cell electropherogram taken under this separation condition is shown in Fig. 3D and d. Peak dispersion was reduced and peak efficiencies were consistent with previous work [31], averaging between 400,000 and 600,000 theoretical plates (Fig. 4). The improvement in peak efficiencies due to dH_2O likely occurred because of the removal of local regions of high ionic strength that are produced during lysis as a result of dilution or sample stacking. While manipulations of buffer content have been used to stack whole fungal cells within a capillary [56], and lower ionic strength solutions were used to improve detection limits for contents isolated from a single sea slug neuron [57], to our knowledge this is the first report of the use of field amplified sample stacking in the analysis of the contents within intact single mammalian cells.

GM1-BODIPY-FL and GM2-BODIPY-FL were baseline resolved under this condition ($R=1.9+0.2$, $N=5$). Several higher order GSL species were detected in both channels, showing that GM1-BODIPY-FL and GM3-BODIPY-TMR both underwent anabolism. The traditional running condition of bracketing a single dPC12 cell suspended in PBS between two plugs of 1% SDS was, in fact, unable to resolve these species; the use of the traditional method could have lead researchers to reach improper biological conclusions regarding GSL metabolism in vitro.

If the ionic strength of single cells/single cell suspensions were too high to allow for proper single cell separations, lowering the ionic strength of the TCS-α running buffer should worsen the separation and increasing the ionic strength of the TCS-α running buffer should improve the quality of the separation. A single dPC12 cell suspended in PBS was aspirated into a capillary and separated in a buffer consisting of 25 mM TRIS, 25 mM CHES, 20 mM SDS, and 5 mM α-CD (Fig. 2E). A representative two-color single cell electropherogram is shown in Fig. 3E and e under this condition. Compared to the normal TCS-α running buffer of higher ionic strength (condition B shown in Fig. 3B and b), peaks were excessively distorted, showing low peak efficiencies (Fig. 4) and poor resolution. Migration times were approximately 2 min shorter due to the increased electric field of the lower ionic strength running buffer.

Next, a single dPC12 cell suspended in PBS was aspirated into a capillary and its contents were separated using a buffer consisting of 250 mM TRIS, 250 mM CHES, 20 mM SDS, and 5 mM α-CD (Fig. 2F) giving a representative two-color single cell electropherogram shown in Fig. 3F and f. Unlike condition B, peaks were nearly symmetrical with several catabolic and anabolic products easily detected. Peak efficiencies in the higher ionic strength TCS-α buffer were significantly greater than condition B for both GM1-BODIPY-FL and Cer-BODIPY-TMR as shown in Fig. 4 ($P=0.007$ and 0.001, respectively, Student's t-test). While the peak efficiencies were not as high as a single dPC12 cell diluted in dH_2O (condition D shown in Fig. 3D and d), the resolution between GM1-BODIPY-FL and GM2-BODIPY-FL was comparable ($R=2.1+0.1$, $N=7$). The migration times were significantly longer due to the lower electric field of the higher ionic strength buffer.

Finally, two separation conditions were combined in an effort to maximize the quality of the separation. Single dPC12 cells suspended in PBS were diluted in dH_2O and separated with a running buffer consisting of 250 mM TRIS, 250 mM CHES, 20 mM SDS, and 5 mM α-CD (Fig. 2G). A representative two-color single cell electropherogram for this condition is shown in Fig. 3G and g. Peaks shapes were Gaussian and peak efficiencies for GSLs in both channels averaged approximately 200,000 theoretical plates (Fig. 4). These peak efficiencies were lower than those measured with single dPC12 cells diluted in dH_2O and run in the normal TCS-α buffer (condition D), the total run time was longer, but there was a gain in resolution. The resolution between GM1-BODIPY-FL and GM2-BODIPY-FL was $3.7+0.3$, significantly higher than condition D ($P=0.001$, Student's t-test).

The improvement in resolution was so dramatic that several other peaks were detected of unknown identity. Some of these species may be the other metabolites shown in Fig. 1A not previously detected. These peaks may also be other GSL species; dPC12 cells are known to express even more complex fucose-containing GSLs [58–60]. New fluorescent GSL standards will need to be synthesized [32] to identify these unknown peaks.

3.3. Manipulation of ionic strength in the 10/35/5 buffer system

Peak dispersion has not been reported in previous analyses of GSL metabolism in single At-T20 pituitary cells, cerebellar granule neurons, or glia [31,48], but there is a critical difference between previous work and this work. GSL metabolism was characterized using the 10/35/5 running buffer. To assess the quality of 10/35/5 running buffer on single dPC12 cell separations, single dPC12 cells suspended in PBS were aspirated into a capillary and the contents were separated using the 10/35/5 buffer. A representative two-color single cell electropherogram is shown in Fig. 5A. Unlike single dPC12 cells suspended in PBS and separated using 100 mM TRIS, 100 mM CHES, 20 mM SDS, and 5 mM α-CD (Figs. 2, 3B and b), only a small amount of fronting was recorded and efficiencies ranged between 400,000 and 600,000 theoretical plates (Fig. 5C), consistent with earlier data [31].

Unlike the separations in the TCS-α buffers, the structure of the BODIPY fluorophore influenced the migration behavior of the fluorescent GSLs in the 10/35/5 buffer. As an example, the Cer-BODIPY metabolites in both channels migrated at different times to a greater degree in the 10/35/5 buffer than in any of the TCS-α buffer formulations. This result could confound proper analyte identification in single cell separations conducted in 10/35/5 with multi-channel laser-induced fluorescence detection. Peaks are identified by either spiking in or comigration with known single analyte standards. A buffer that allows species with the same GSL headgroup but different fluorophores (ex: Cer-BODIPY-FL and Cer-BODIPY-TMR) to comigrate will only need one lipid standard, regardless of the fluorophore, for proper identification of a particular metabolic product. Conversely, a buffer such as 10/35/5 that does not allow these species to comigrate would need standards available for each GSL with each fluorophore utilized for proper identification of all metabolic products. Fluorescent GSL species are individually synthetically and chemoenzymatically prepared so this would require tremendous time and effort for single cell electrophoretic separations using multicolor laser-induced fluorescence detection.

The migration order of the fluorescently labeled GSLs differed between the TCS-α and 10/35/5 buffers (compare Figs. 3 and 5). While both 10/35/5 and TCS-α provide an MECC-based separation, the mechanism of separation is different between these two buffers, giving differences in GSL metabolite migration order [38]. First, GSLs are known to form complexes with borate anions during electrophoretic separations [34]. Second, the degree of interaction between GSLs and cyclodextrins is highly dependent on the cyclodextrin structure [33]. Third, the degree to which SDS aids in the separation of anionic lipids depends on the buffer used [33,38,61]. For example, the addition of SDS to a borate-based buffer could not separate amino-group containing phospholipids [61], but SDS offered the best separation of GSLs in a TRIS/CHES-based buffer system [38]. Taken together, these observations could explain why GSL peaks appeared fronted for the TCS-α buffer, contrary to previous work in 10/35/5 buffer.

Despite the differences in separation mechanism given by the 10/35/5 buffer compared to the TCS-α formulation, a final separation condition was tested to determine if a reduction of ionic strength of the single cell/single cell suspension could be used more broadly as a tool to improve the quality of single cell separations in general. Single dPC12 cells suspended in PBS were diluted with dH_2O, aspirated into the capillary, and separated using the 10/35/5 running buffer. A representative two-color single cell electropherogram is shown in Fig. 5B. The small peak dispersions shown in Fig. 5A were eliminated. Peak efficiencies significantly improved for both GM1-BODIPY-FL and Cer-BODIPY-TMR as shown in Fig. 5C ($P=0.001$ and 0.003, respectively, Student's t-test), averaging between 800,000 and 1,000,000 theoretical plates. This result demonstrates that low ionic strength injection conditions can be utilized more broadly for improved single cell separations.

4. Conclusions

Here we presented methodology for improved single cell electrophoretic separations. Single neuronal-like dPC12 cells were

aspirated and fluorescent GSLs were electrophoresed under different experimental conditions. Cellular ionic strength was determined to play an essential role in obtaining efficient separations. Diluting a suspension of dPC12 cells in dH_2O increased GSL peak efficiencies approximately two-fold in a borate/deoxycholate/methyl-β-CD running buffer and nearly an order of magnitude in a TRIS/CHES/SDS/α-CD running buffer. Diluting the cell suspension in dH_2O before single cell aspiration and utilizing a running buffer of higher ionic strength gave the best balance between improved peak efficiency and resolution. The improved resolution allowed for the detection of analytes previously uncharacterized at the single cell level. This work demonstrates that the manipulation of ionic strength can provide another essential tool for improving electrophoretic separations on the single cell level.

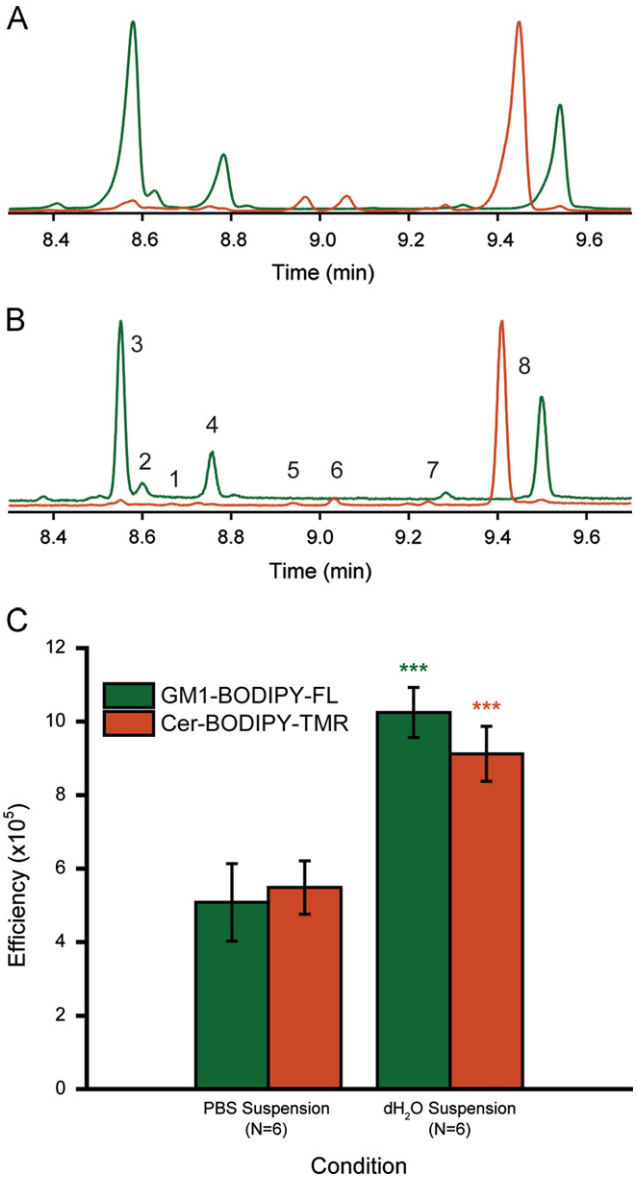

Fig. 5. Two-color metabolic cytometry of single dPC12 cells in the 10/35/5 buffer. (A) A single dPC12 cell suspended in PBS was separated using the 10/35/5 buffer. (B) A single dPC12 cell diluted in dH_2O was separated using the 10/35/5 buffer. In each two-color electropherogram, the abscissa represents migration time while the ordinate is in units of fluorescence (Hz). Green and orange traces correspond to the BODIPY-FL and BODIPY-TMR channels, respectively. A running voltage of 18 kV was used for all separations. The numbered labels correspond to GSLs GT1a/b (1), GD1a/b (2), GM1 (3), GM2 (4), GM3 (5), LacCer (6), GlcCer (7), and Cer (8). (C) Peak efficiencies for GM1-BODIPY-FL (green) and Cer-BODIPY-TMR (orange) for both conditions. Asterisks correspond to a significant increase ($P<0.005$) in peak efficiency for single dPC12 cells diluted in dH_2O compared to PBS. *N* is the number of single cells analyzed with each separation condition. (For interpretation of the references to color in this figure legend, the reader is referred to the web version of this article.)

Acknowledgments

This work was supported by the National Institutes of Health (R01NS061767).

References

[1] H.B. Yin, D. Marshall, Curr. Opin. Biotechnol. 23 (2012) 110–119.
[2] M.A. Walling, J.R.E. Shepard, Chem. Soc. Rev. 40 (2011) 4049–4076.
[3] R.A. Wallingford, A.G. Ewing, Anal. Chem. 60 (1988) 1972–1975.
[4] R.T. Kennedy, M.D. Oates, B.R. Cooper, B. Nickerson, J.W. Jorgenson, Science 246 (1989) 57–63.
[5] S. Hu, J. Jiang, L.M. Cook, D.P. Richards, L. Horlick, B. Wong, N.J. Dovichi, Electrophoresis 23 (2002) 3136–3142.
[6] G.K. Shoemaker, J. Lorieau, L.H. Lau, C.S. Gillmor, M.M. Palcic, Anal. Chem. 77 (2005) 3132–3137.
[7] S.N. Arkhipov, M. Berezovski, J. Jitkova, S.N. Krylov, Cytom. Part A 63A (2005) 41–47.
[8] H. Zhang, W.R. Jin, Electrophoresis 25 (2004) 1090–1095.
[9] X. Liu, L. Ma, H.F. Zhang, Y.T. Lu, J. Chromatogr. B 808 (2004) 241–247.
[10] N.J. Dovichi, S. Hu, Curr. Opin. Chem. Biol. 7 (2003) 603–608.
[11] J.L. Zabzdyr, S.J. Lillard, TRAC—Trend. Anal. Chem. 20 (2001) 467–476.
[12] S.D. Gilman, A.G. Ewing, Anal. Chem. 67 (1995) 58–64.
[13] R.L. Schnaar, Brain Glycolipids: Insights from Genetic Modifications of Biosynthetic Enzymes, in: M. Fukuda, U. Rutishauser, R.L. Schnaar (Eds.), Neuroglycobiology, Oxford University Press, Oxford, New York, 2005, pp. 95–113.
[14] R. De Maria, L. Lenti, F. Malisan, F. d'Agostino, B. Tomassini, A. Zeuner, M.R. Rippo, R. Testi, Science 277 (1997) 1652–1655.
[15] R. De Maria, L. Lenti, F. Malisan, F. d'Agostino, B. Tomassini, A. Zeuner, M.R. Rippo, R. Testi, Science 280 (1998) 359.
[16] S. Hakomori, J. Biol. Chem. 265 (1990) 18713–18716.
[17] S. Spiegel, A.H. Merrill, FASEB J. 10 (1996) 1388–1397.
[18] F.J. Roisen, H. Bartfeld, R. Nagele, G. Yorke, Science 214 (1981) 577–578.
[19] K. Obata, M. Oide, S. Handa, Nature 266 (1977) 369–371.
[20] G. Ferrari, M. Fabris, A. Gorio, Dev. Brain Res. 8 (1983) 215–221.
[21] S.F. Martin, S. Chatterjee, Methods Enzymol. 363 (2003) 284–299.
[22] K. Sango, S. Yamanaka, A. Hoffmann, Y. Okuda, A. Grinberg, H. Westphal, M.P. McDonald, J.N. Crawley, K. Sandhoff, K. Suzuki, R.L. Proia, Nat. Genet. 11 (1995) 170–176.
[23] F.M. Platt, T.D. Butters, Biochem. Pharmacol. 56 (1998) 421–430.
[24] Y.H. Xu, S. Barnes, Y. Sun, G.A. Grabowski, J. Lipid Res. 51 (2010) 1643–1675.
[25] S.U. Walkley, M.T. Vanier, Biochim. Biophys. Acta—Mol. Cell Res. 2009 (1793) 726–736.
[26] S.N. Krylov, Z. Zhang, N.W. Chan, E. Arriaga, M.M. Palcic, N.J. Dovichi, Cytometry 37 (1999) 14–20.
[27] N.G. Lipsky, R.E. Pagano, Proc. Natl. Acad. Sci. USA 80 (1983) 2608–2612.
[28] R.E. Pagano, O.C. Martin, H.C. Kang, R.P. Haugland, J. Cell Biol. 113 (1991) 1267–1279.
[29] T. Shiraishi, M. Hiraiwa, Y. Uda, Glycoconjugate J. 10 (1993) 170–174.
[30] R.E. Pagano, R. Watanabe, C. Wheatley, M. Dominguez, Methods Enzymol. 312 (2000) 523–534.
[31] D.C. Essaka, J. Prendergast, R.B. Keithley, M.M. Palcic, O. Hindsgaul, R.L. Schnaar, N.J. Dovichi, Anal. Chem. 84 (2012) 2799–2804.
[32] R.B. Keithley, A.S. Rosenthal, D.C. Essaka, H. Tanaka, Y. Yoshimura, M.M. Palcic, O. Hindsgaul, N.J. Dovichi, Analyst 138 (2013) 164–170.
[33] Y.S. Yoo, Y.S. Kim, G.J. Jhon, J. Park, J. Chromatogr. A 652 (1993) 431–439.
[34] D.D. Ju, C.C. Lai, G.R. Her, J. Chromatogr. A 779 (1997) 195–203.
[35] Z. Yu, Y. Chen, G. Xu, L. Chang, J. Liq. Chromatogr. Relat. Technol. 21 (1998) 349–360.
[36] Y.B. Liu, K.F. Chan, Electrophoresis 12 (1991) 402–408.
[37] B. Ulrich-Bott, H. Wiegandt, J. Lipid Res. 25 (1984) 1233–1245.
[38] S.A. Sarver, R.B. Keithley, D.C. Essaka, H. Tanaka, Y. Yoshimura, M.M. Palcic, O. Hindsgaul, N.J. Dovichi, J. Chromatogr. A 1229 (2012) 268–273.
[39] C. Cecala, J.V. Sweedler, Analyst 137 (2012) 2922–2929.
[40] B.L. Hogan, E.S. Yeung, Anal. Chem. 64 (1992) 2841–2845.
[41] S.N. Krylov, D.A. Starke, E.A. Arriaga, Z.R. Zhang, N.W.C. Chan, M.M. Palcic, N.J. Dovichi, Anal. Chem. 72 (2000) 872–877.
[42] L.A. Greene, A.S. Tischler, Proc. Natl. Acad. Sci. USA 73 (1976) 2424–2428.
[43] R.P. Haugland, The Handbook: A Guide to Fluorescent Probes and Labeling Technologies, 10th ed., Invitrogen Corporation, USA, 2005.
[44] D.C. Essaka, J. Prendergast, R.B. Keithley, O. Hindsgaul, M.M. Palcic, R.L. Schnaar, N.J. Dovichi, Neurochem. Res. 37 (2012) 1308–1314.
[45] K. Sobhani, D.A. Michels, N.J. Dovichi, Appl. Spectrosc. 61 (2007) 777–779.
[46] C.D. Whitmore, D. Essaka, N.J. Dovichi, Talanta 80 (2009) 744–748.
[47] J.P. Foley, J.G. Dorsey, Anal. Chem. 55 (1983) 730–737.

[48] C.D. Whitmore, O. Hindsgaul, M.M. Palcic, R.L. Schnaar, N.J. Dovichi, Anal. Chem. 79 (2007) 5139–5142.
[49] G. Ocvirk, H. Salimi-Moosavi, R.J. Szarka, E.A. Arriaga, P.E. Andersson, R. Smith, N.J. Dovichi, D.J. Harrison, Proc. IEEE 92 (2004) 115–125.
[50] Applied Biosystems, DNA-*ZAP*™ Solutions. Manual 9890M, 2008.
[51] P.S. Belton, H. Sørensen, S. Sørensen, C. Bjergegaard, S. Michaelsen, Chromatography and Capillary Electrophoresis in Food Analysis, Royal Society of Chemistry, Cambridge, UK, 1999.
[52] E.R. Kandel, J.H. Schwartz, T.M. Jessell, Principles of Neural Science, 4th ed., McGraw-Hill, Health Professions Division, New York, 2000.
[53] T.P. Roddy, D.M. Cannon, S.G. Ostrowski, N. Winograd, A.G. Ewing, Anal. Chem. 74 (2002) 4020–4026.
[54] C.-X. Zhang, W. Thormann, Anal. Chem. 68 (1996) 2523–2532.
[55] H.F. Fang, T.L. Vickrey, B.J. Venton, Anal. Chem. 83 (2011) 2258–2264.
[56] A.W. Lantz, B. Bisha, M.Y. Tong, R.E. Nelson, B.F. Brehm-Stecher, D.W. Armstrong, Electrophoresis 31 (2010) 2849–2853.
[57] J.S. Page, S.S. Rubakhin, J.V. Sweedler, Anal. Chem. 74 (2002) 497–503.
[58] R.U. Margolis, M. Mazzulla, L.A. Greene, R.K. Margolis, FEBS Lett. 172 (1984) 339–342.
[59] K.M. Walton, K. Sandberg, T.B. Rogers, R.L. Schnaar, J. Biol. Chem. 263 (1988) 2055–2063.
[60] G.A. Schwarting, A. Gajewski, L. Barbero, A.S. Tischler, D. Costopoulos, Neuroscience 19 (1986) 647–656.
[61] Z. Le, S.N. Krylov, S. Hu, N.J. Dovichi, J. Chromatogr. A 894 (2000) 129–134.